Inorg. Chem. **1987**, *26*, 3333–3339

Contribution from the Department of Chemistry,
The University of Alberta, Edmonton, Alberta, Canada T6G 2G2

Diphosphine-Bridged Binuclear Polyhydride Complexes of Iridium and the Structure of $[Ir_2(H)(CO)_2(\mu\text{-}H)_2(Ph_2PCH_2PPh_2)_2][Cl]\cdot 1.2CH_2Cl_2$

Robert McDonald, Bruce R. Sutherland, and Martin Cowie*

Received November 24, 1986

The reaction of *trans*-$[IrCl(CO)(DPM)]_2$ (DPM = bis(diphenylphosphino)methane) with $NaBH_4$ under an H_2 atmosphere yields the binuclear tetrahydride $[Ir_2(H)_4(CO)_2(DPM)_2]$ (**3**). Addition of strong acid ($HBF_4\cdot Et_2O$ or CF_3CO_2H) to this complex under an H_2 atmosphere causes a reversible rearrangement to the isomer $[Ir_2(H)_2(CO)_2(\mu\text{-}H)_2(DPM)_2]$ (**4**). If the addition of $HBF_4\cdot Et_2O$ is performed under an N_2 atmosphere, the cationic trihydride $[Ir_2(H)(CO)_2(\mu\text{-}H)_2(DPM)_2][BF_4]$ (**5a**) is isolated instead. This compound is also formed from the reaction of **3** with $Ph_3C^+BF_4^-$. Protonation of **5** with $HBF_4\cdot Et_2O$ yields the dicationic tetrahydride $[Ir_2(H)_2(CO)_2(\mu\text{-}H)_2(DPM)_2][BF_4]_2$ (**8**), and deprotonation of **5** by $KOC(CH_3)_3$ yields the dihydride $[Ir_2(CO)_2(\mu\text{-}H)_2(DPM)_2]$ (**7**). Compound **3** reacts with CH_2Cl_2 or $CHCl_3$, yielding $[Ir_2(H)(CO)_2(\mu\text{-}H)_2(DPM)_2][Cl]$ (**5b**), by exchange of one hydride ligand for Cl^-. Compound **5b** crystallizes from CH_2Cl_2 with two molecules of solvent in the monoclinic space group $P2_1/n$ with $a = 12.794$ (4) Å, $b = 20.468$ (5) Å, $c = 20.433$ (8) Å, $\beta = 91.58$ (4)°, and $Z = 4$. The structure refined to $R = 0.080$ and $R_w = 0.102$ on the basis of 3543 unique observed reflections and 241 parameters varied. Although the hydride ligands were not located, their positions can be inferred from the positions of the other ligands and from the spectroscopic evidence. Two hydrides bridge the Ir–Ir bond on opposite faces of the dimer and one is terminally bound. This terminal hydride causes the adjacent carbonyl to bend off the Ir–Ir axis such that the corresponding Ir–Ir–CO angle is 129 (1)°. By contrast, the other carbonyl ligand is aligned almost parallel to the Ir–Ir bond (Ir–Ir–CO angle = 163 (1)°). The metal–metal distance is 2.855 (2) Å.

Introduction

Group 8 transition-metal hydrides are among the most studied complexes in organometallic chemistry[1] and have been implicated in such catalytic processes as olefin hydrogenations,[2] hydroformylations[3] and the water gas shift reaction.[4] Our interests have been in extending this chemistry to complexes involving two adjacent metals, in order to determine whether the metals can react with substrate molecules in a cooperative manner. As part of this study we have recently investigated a series of binuclear, DPM-bridged iridium hydrides (DPM = $Ph_2PCH_2PPh_2$) as potential models for multicenter catalysts[5,6] and now report an extension of these studies.

One approach to the preparation of metal hydrides is by the direct reaction of H_2 with metal complexes. Such hydride species have obvious relevance to catalytic processes that utilize H_2 as a reactant. Some of our recent work in this area is the basis of a previous report.[6] A second approach, which will form the focus of this paper, involves the use of borohydride reagents to replace halide ligands by the more catalytically interesting hydrido ligand. Part of our strategy in this latter approach was to prepare complexes in which as many of the ligands as possible were chemically active. We therefore set out to prepare complexes such as *trans*-$[IrH(CO)(DPM)]_2$, a binuclear iridium analogue of $[RhH(CO)(PPh_3)_2]$, a catalytically active species in olefin hydrogenation and hydroformylation reactions.[2,3] Herein we present the results of this study.

Experimental Section

All solvents were appropriately dried and distilled prior to use and were stored under dinitrogen. Reactions were performed under standard Schlenk conditions using dinitrogen that had been previously passed through columns containing Ridox and 4A molecular sieves to remove traces of oxygen and water, respectively. Hydrated iridium(III) chloride was obtained on loan from Johnson Matthey and bis(diphenylphosphino)methane (DPM) was purchased from Strem Chemicals. Carbon monoxide was obtained from Matheson and used as received. *trans*-$[IrCl(CO)(DPM)]_2$ (**1**)[7] and $[Ir_2(CO)_2(\mu\text{-}H)(\mu\text{-}CO)(DPM)_2][BF_4]$ (**2**)[5] were prepared by previously reported procedures. Variable-temperature $^{31}P\{^1H\}$ NMR spectra were run on either a Bruker WH-400 spectrometer operating at 161.9 MHz or a Bruker HFX-90 spectrometer operating at 36.43 MHz. In the former case acetone-d_6 was used as an internal lock, whereas an external acetone-d_6 lock was used in the latter; chemical shifts were referenced to 85% H_3PO_4. ^1H NMR spectra were recorded on either a Bruker WH-200 or Bruker WH-400 spectrometer at room temperature. Infrared spectra were run on a Nicolet 7199 Fourier transform interferometer either as solids in Nujol mulls on KBr plates or as solutions in NaCl cells with 0.5-mm path length windows. Analyses were performed by the microanalytical service within the department.

Preparation of Compounds. (a) $[Ir_2(H)_4(CO)_2(DPM)_2]$ (3). An atmosphere of hydrogen was placed over a slurry of *trans*-$[IrCl(CO)(DPM)]_2$ (**1**) (200 mg, 0.156 mmol) and $NaBH_4$ (25 mg, 0.661 mmol) in THF (20 mL). The mixture was stirred for 8 h during which time all of **1** was consumed, producing a bright yellow solution. A 500-μL aliquot of degassed water was then added to the mixture to destroy the excess borohydride, resulting in significant gas evolution. When this subsided (ca. 30 s), the solution was taken to dryness under vacuum, resulting in the isolation of a bright yellow powder. The solid was redissolved in THF (20 mL) and was then filtered under nitrogen, yielding a clear bright yellow solution. The volume was reduced to 5 mL under vacuum, 20 mL of hexanes added, and the solution stored overnight at −15 °C. This yielded **3** as a yellow microcrystalline product in about 75% yield. Spectroscopic parameters for this and all subsequent compounds are given in Table I. When dissolved in CH_2Cl_2, compound **3** proved to be nonconducting (Λ (10^{-3} M) = 4.0 Ω^{-1} cm^2 mol^{-1}).[8] Anal. Calcd for $C_{52}H_{48}Ir_2O_2P_4$: C, 51.48; H, 3.99. Found: C, 51.61; H, 4.08.

(b) $[Ir_2(H)_2(CO)_2(\mu\text{-}H)_2(DPM)_2]$ (4). To a solution of **3** in CH_2Cl_2 (150 mg, 0.124 mmol in 10 mL) under an atmosphere of hydrogen was added 1 equiv of $HBF_4\cdot Et_2O$ (17.8 μL, 0.124 mmol), causing an immediate color change to pale yellow. Although this species was characterized in solution (see Table I), all attempts to obtain it as a solid resulted in a mixture of products, the major product being compound **5** (vide infra).

(c) $[Ir_2(H)(CO)_2(\mu\text{-}H)_2(DPM)_2][BF_4]\cdot CH_2Cl_2$ (5a). Method A. To a solution of **3** in CH_2Cl_2 under an atmosphere of nitrogen (150 mg, 0.124 mmol in 10 mL) was added 1 equiv of $HBF_4\cdot Et_2O$ (17.8 μL, 0.124 mmol), causing the solution color to change to light yellow. The solution was then stirred for 24 h under a very slow nitrogen stream during which time the color deepened to golden yellow. The volume was reduced to 5 mL under nitrogen, and then 25 mL of Et_2O was added, causing the precipitation of a golden yellow solid in 90% yield after recrystallization from CH_2Cl_2/Et_2O. Compound **5a** proved to be a 1:1 electrolyte in CH_2Cl_2 (Λ (10^{-3} M) = 45.7 Ω^{-1} cm^2 mol^{-1}). Anal. Calcd for $BC_{53}Cl_2F_4H_{49}Ir_2O_2P_4$: C, 45.99; H, 3.57; Cl, 5.12. Found: C, 45.60; H, 3.59; Cl, 5.09.

---

(1) Muetterties, E. L., Ed. *Transition Metal Hydrides*; Marcel Dekker: New York, 1971 and references therein.
(2) James, B. R. *Homogeneous Hydrogenation*; Wiley: New York, 1974.
(3) Pruett, R. L. *Adv. Organomet. Chem.* **1979**, *17*, 1.
(4) Yoshida, T.; Okano, T.; Ueda, Y.; Otsuka, S. *J. Am. Chem. Soc.* **1981**, *103*, 3411 and references therein.
(5) Sutherland, B. R.; Cowie, M. *Organometallics* **1985**, *4*, 1637.
(6) Sutherland, B. R.; Cowie, M. *Organometallics* **1985**, *4*, 1801.
(7) Sutherland, B. R.; Cowie, M. *Inorg. Chem.* **1984**, *23*, 2324.
(8) Typically a 1:1 electrolyte such as $[Rh_2(CO)_2(\mu\text{-}Cl)(\mu\text{-}CO)(DPM)_2][BF_4]$ gives a value of ca. 45 Ω^{-1} cm^2 mol^{-1}. See also: Geary, W. J. *Coord. Chem. Rev.* **1971**, *7*, 81.

0020-1669/87/1326-3333$01.50/0

Table I. Spectral Data[a]

compd	IR, cm^{-1}		NMR	
	solid[b]	solution[c]	$\delta(^{31}P\{^1H\})$[d]	$\delta(^1H)$[e]
$[Ir_2(H)_4(CO)_2(DPM)_2]$ (**3**)	1933 (vs), 1890 (vs)[f] 2076 (m), 2107 (w)[g]	1944 (vs, br), 1899 (st)[f] 2061 (m, br), 2110 (br, sh)[g]	−3.4 (s)	7.56–7.05 (mult, 40 H), 5.84 (mult, 2 H), 4.07 (mult, 2 H), −10.94 (mult, 2 H, $^2J_{H-H}$ = 4.7 Hz), −11.39 (mult, 2 H, $^2J_{H-H}$ = 4.7 Hz)
$[Ir_2(H)_2(CO)_2(\mu-H)_2(DPM)_2]$ (**4**)	*h*	*i*	−6.6 (s)	7.65–7.33 (mult, 40 H), 4.96 (s, br, 4 H), −10.46 (q, br, 2 H, $^2J_{P-H} \sim 12$ Hz), −13.42 (br, 2 H)
$[Ir_2(H)(CO)_2(\mu-H)_2(DPM)_2][BF_4]$ (**5a**)	1959 (vs)[f] 2049 (st)[g]	1966 (br, vs)[f] 2059 (st)[g]	15.1, −0.7 (mult)	7.65–7.16 (mult, 40 H), 4.91 (mult, 2 H), 3.96 (mult, 2 H), −10.11 (mult, 1 H), −10.34 (mult, 1 H), −11.13 (tr, 1 H, $^2J_{P-H}$ = 14.2 Hz)
$[Ir_2(H)(CO)_2(\mu-H)_2(DPM)_2][Cl]$ (**5b**)	1956 (vs)[f] 2043 (s)[g]	1969 (vs)[f] 2056 (s)[g]	14.9, −1.0 (mult)	7.59–7.17 (mult, 40 H), 4.86 (br, 2 H), 3.97 (br, 2 H), −10.23 (br, 1 H), −10.49 (br, 1 H), −11.18 (tr, 1 H, $^2J_{P-H}$ = 14.3 Hz)
$[Ir_2(CO)_2(\mu-H)_2(DPM)_2]$ (**7**)	*h*	1909 (vs)[f]	12.9 (s)	7.68–7.16 (mult, 40 H), 4.56 (br, 4 H), −10.12 (q, 2 H, $^2J_{P-H}$ = 6.6 Hz)[j]
$[Ir_2(H)_2(CO)_2(\mu-H)_2(DPM)_2][BF_4]_2$ (**8**)	2071 (vs)[f] 2022 (w)[g]	2084 (vs)[f] 2039 (w)[g]	9.0 (s)	7.67–7.29 (mult, 40 H), 4.96 (mult, 4 H), −9.20 (mult, 2 H), −19.22 (mult, 2 H)[k]
$[Ir_2(CO)_4(\mu-H)(DPM)_2][BF_4]$ (**9**)	*h*	1998 (st), 1981 (vs), 1959 (vs)[f]	−9.6 (s)	7.82–7.24 (mult, 40 H), 5.02 (br, 4 H), −9.95 (q, 1 H, $^2J_{P-H}$ = 9.4 Hz)[k]

[a] Abbreviations used: w = weak, m = medium, st = strong, vs = very strong, br = broad, s := singlet, mult = multiplet, tr = triplet, q = quintet. [b] Nujol mull on KBr disk. [c] CH_2Cl_2 solution in NaCl cells. [d] Vs. 85% H_3PO_4, −40 °C. [e] Vs. TMS, 25 °C; in CD_2Cl_2 solvent unless otherwise noted. [f] ν(CO). [g] ν(Ir–H). [h] Not isolable in solid state. [i] Reacts with IR plates. [j] In THF-d_8. [k] In CD_3NO_2.

Method B. To a solution of **3** in CH_2Cl_2 (150 mg, 0.124 mmol in 5 mL) was added dropwise 1 equiv of $Ph_3C^+BF_4^-$ (37.3 mg, 0.124 mmol) in 2 mL of CH_2Cl_2, producing a rapid color change from bright yellow to dark golden yellow. The solution volume was reduced to 5 mL under an N_2 flow, and the addition of 25 mL of Et_2O resulted in the precipitation of a golden yellow solid which was in all its properties identical with that prepared by method A.

(d) $[Ir_2(H)(CO)_2(\mu-H)_2(DPM)_2][Cl]\cdot 2CH_2Cl_2$ (5b). A solution of **3** in $CHCl_3$ (100 mg, 0.082 mmol in 5 mL), under an N_2 atmosphere, was allowed to stir for 20 min during which time the color changed from bright yellow to golden yellow. The solution was taken to dryness under a rapid N_2 flow leaving a golden brown solid. Recrystallization from CH_2Cl_2/Et_2O gave a golden yellow powder in 71% yield. Compound **5b** proved to be weakly conducting in CH_2Cl_2 (Λ (10^{-3} M) = 10.4 Ω^{-1} cm^2 mol^{-1}) and in nitromethane (Λ (10^{-3} M) = 26.2 Ω^{-1} cm^2 mol^{-1}). Anal. Calcd for $C_{54}Cl_5H_{51}Ir_2O_2P_4$: C, 45.75; H, 3.63; Cl, 12.51. Found: C, 45.82; H, 3.65; Cl, 12.48.

(e) $[Ir_2(CO)_2(\mu-H)_2(DPM)_2]$ (7). A THF solution of **5a** (100 mg, 0.072 mmol in 10 mL) under N_2 was chilled to 0 °C and a THF solution of $KOC(CH_3)_3$ (8.6 mg, 0.077 mmol in 1 mL) was added. The solution color immediately changed from golden yellow to deep red. Attempts to crystallize this material led to a number of decomposition products, but this species has been characterized in solution by IR and NMR (^1H, $^{31}P\{^1H\}$) spectroscopy.

(f) $[Ir_2(H)_2(CO)_2(\mu-H)_2(DPM)_2][BF_4]_2$ (8). To a solution of **5a** in CH_2Cl_2 (150 mg, 0.108 mmol in 10 mL) was added an excess of $HBF_4\cdot Et_2O$ (45.0 μL, 0.313 mmol) under a slow N_2 stream, causing the immediate precipitation of a white solid. Complete precipitation was induced by the addition of 20 mL of Et_2O. The solid was collected and washed with a further 10-mL portion of Et_2O and finally dried in vacuo for 2 h. Typical isolated yields after crystallization from CH_2Cl_2/Et_2O were about 90%. Compound **8** proved to be a 2:1 electrolyte in nitromethane (Λ (10^{-3} M) = 158.2 Ω^{-1} cm^2 mol^{-1}). Anal. Calcd for $B_2C_{52}F_8H_{48}Ir_2O_2P_4$: C, 45.04; H, 3.49. Found: C, 45.12; H, 3.32.

(g) $[Ir_2(CO)_4(\mu-H)(DPM)_2][BF_4]$ (9). Method A. A solution of $[Ir_2(CO)_2(\mu-H)(\mu-CO)(DPM)_2][BF_4]$ (**2**) was prepared by adding 1 equiv (11.6 μL, 0.081 mmol) of $HBF_4\cdot Et_2O$ to a CH_2Cl_2 solution of $[Ir_2(CO)_3(DPM)_2]$ (100 mg, 0.081 mmol in 5 mL) under N_2.[5] An atmosphere of CO was then placed over this solution, causing a change of color from deep red-purple to medium red-orange. The solution was taken to dryness under a CO stream, leaving a light red-brown residue. Recrystallization from CH_2Cl_2/Et_2O produced a pale orange powder that immediately turned pink when the CO atmosphere was removed, thus precluding its elemental analysis; however, this species has been characterized in solution by IR and NMR (^1H, $^{31}P\{^1H\}$) spectroscopy. Furthermore, the species giving rise to the pink color was identified by spectroscopic techniques as **2**.

Method B. A solution of $[Ir_2(CO)_4(DPM)_2]$ was prepared by bubbling CO through a CH_2Cl_2 solution of $[Ir_2(CO)_3(DPM)_2]$ (100 mg, 0.081 mmol in 5 mL).[5] One equivalent (11.6 μL, 0.081 mmol) of $HBF_4\cdot Et_2O$ was added, causing a color change from bright yellow to red-orange. The product was found in its spectroscopic properties to be identical with that prepared by method A.

Preparation of Deuteride Complexes. The deuteride analogues of compounds **3**–**5** were prepared as reported above except that $NaBD_4$, D_2O, and D_2 were substituted for $NaBH_4$, H_2O, and H_2 in the appropriate places.

Reaction of $[Ir_2(H)(CO)_2(\mu-H)_2(DPM)_2][BF_4]$ (5a) with $NaBH_4$. A suspension of **5a** (150 mg, 0.108 mmol) and $NaBH_4$ (25 mg, 0.661 mmol) in 10 mL of THF was stirred for 24 h during which time the solid dissolved and a bright yellow solution formed. A 500-μL aliquot of degassed water was then added to the solution to destroy the excess borohydride, and the solution was taken to dryness in vacuo, leaving a bright yellow powder. The solid was redissolved in THF and filtered under N_2, yielding a bright yellow solution. The addition of 30 mL of hexanes followed by concentration of the solution under vacuum resulted in the precipitation of a yellow microcrystalline product, which was identical with **3** in all of its spectroscopic properties.

Attempted Reactions of $[Ir_2(H)_4(CO)_2(DPM)_2]$ (3) and $[Ir_2(H)(CO)_2(\mu-H)_2(DPM)_2][BF_4]$ (5a) with Nitrogen Bases. To a solution of **3** in CH_2Cl_2 (150 mg, 0.116 mmol) in 10 mL) was added an excess of Proton Sponge[9] (Aldrich) (75.0 mg, 0.350 mmol) in 2 mL of CH_2Cl_2. The solution was allowed to stir for 24 h with no apparent change. Both $^{31}P\{^1H\}$ NMR and IR spectra after this time showed only starting material, indicating that no reaction had occurred. Similar results were obtained with **5a**. No change in solutions of **3** and **5a** occurred when NEt_3 was used as the base.

Reaction of $[Ir_2(H)_2(CO)_2(\mu-H)_2(DPM)_2][BF_4]_2$ (8) with Proton Sponge.[9] To a suspension of **8** (150 mg, 0.108 mmol) in 10 mL of CH_2Cl_2 was added a solution of 1 equiv of Proton Sponge (23.1 mg, 0.108 mmol) in 2 mL of CH_2Cl_2. A rapid reaction occurred as evidenced by the dissolution of the solid and the formation of a dark yellow solution. Addition of ether to this solution resulted in the precipitation of a golden yellow solid, which was shown to be **5a** on the basis of its infrared and $^{31}P\{^1H\}$ NMR spectra.

Reaction of $[Ir_2(CO)_2(\mu-H)_2(DPM)_2]$ (7) with $HBF_4\cdot Et_2O$. To a solution of **7** in THF (0.062 mmol in 5 mL, prepared in situ from **5a**) was added 1 equiv of $HBF_4\cdot Et_2O$ (0.062 mmol, 8.8 μL), causing an immediate color change from deep red to golden yellow. The product was shown to be **5a** on the basis of its ^1H and $^{31}P\{^1H\}$ NMR spectra.

Reaction of $[Ir_2(CO)_2(\mu-H)_2(DPM)_2]$ (7) with H_2. Hydrogen was bubbled through a THF solution of **7** (0.062 mmol in 5 mL; prepared in situ from **5a**), causing an immediate color change from deep red to yellow. The product was shown to be **3** on the basis of its ^1H and $^{31}P\{^1H\}$ NMR spectra.

Reaction of $[Ir_2(H)_2(CO)_2(\mu-H)_2(DPM)_2][BF_4]_2$ (8) with CO. An atmosphere of CO was placed over a nitromethane solution of **8** (50 mg, 0.036 mmol in 2 mL). Within 15 min, the solution color had changed from golden brown to golden yellow. The product was shown to be $[Ir_2(CO)_4(\mu-H)_2(DPM)_2][BF_4]_2$ on the basis of a comparison of its ^1H and $^{31}P\{^1H\}$ NMR spectra with those of an authentic sample.[5]

---

(9) 1,8-Bis(dimethylamino)naphthalene.

Apparent T_1 Measurements. The apparent relaxation times of the hydride NMR resonances were obtained by inversion–recovery at 25 °C and 400 MHz by using a 180°–t–90° pulse sequence. Delay times were varied from 5 to 800 ms.

X-ray Data Collection

Suitable X-ray diffraction quality crystals of $[Ir_2(H)(CO)_2(\mu\text{-}H)_2(DPM)_2][Cl]$ (**5b**) were obtained by serendipity by the slow diffusion of ether into a CH_2Cl_2 solution of $[Ir_2(H)_4(CO)_2(DPM)_2]$ (**3**) under an N_2 atmosphere. These crystals proved to be indistinguishable from samples of the BF_4^- salt **5a** in all spectroscopic properties apart from those resulting from the BF_4^- group itself. Several crystals were mounted in thin-walled glass capillaries under nitrogen to minimize decomposition. Unit cell parameters were obtained from a least-squares refinement of the setting angles of 25 reflections in the range $13.0° \leqslant 2\theta \leqslant 22.0°$, which were accurately centered on an Enraf-Nonius CAD4 diffractometer using Mo Kα radiation. Since four crystals were used for data collection, the cell parameters reported are those from the best crystal; all others gave similar values. The systematic absences ($h0l$, $h + l$ = odd; $0k0$, k = odd) were consistent with the space group $P2_1/n$ (a nonstandard setting of $P2_1/c$).

Intensity data were collected on a CAD4 diffractometer in the bisecting mode employing the ω–2θ scan technique up to $2\theta = 50.00°$ with graphite-monochromated Mo Kα radiation. Backgrounds were scanned for 25% of the peak width on either end of the peak scan. The crystals proved to be susceptible to decomposition in the X-ray beam as evidenced by the decline of the intensities of three standard reflections monitored every 1 h of exposure time. When these standards dropped to 75% of their original intensity, data collection was stopped and a new crystal was used. Attempts to collect data at low temperature (−40 °C) were unsuccessful since the decomposition was not slowed significantly and crystal movement in the cold stream caused additional difficulties. In all, four different crystals were employed to collect the data. A linear decomposition correction was applied to the data from each crystal. A total of 9461 unique reflections were measured and processed in the usual way with a value of 0.04 used for p;[10] of these 3543 were considered to be observed and were used in subsequent calculations. Absorption corrections were applied to the data by using Gaussian integration.[11] See Table II for pertinent crystal data and details of intensity collection.

Structure Solution and Refinement

The structure was solved in the space group $P2_1/n$ by using standard Patterson and Fourier techniques. All nonhydrogen atoms were ultimately located. In the full-matrix least-squares refinements, the data from each crystal were independently scaled. Atomic scattering factors were taken from Cromer and Waber's tabulation[12] for all atoms except hydrogen, for which the values of Stewart et al.[13] were used. Anomalous dispersion terms[14] for Ir, Cl, and P were included in F_c. The carbon atoms of the phenyl rings were refined as rigid groups having D_{6h} symmetry, C–C distances of 1.392 Å, and independent isotropic thermal parameters. All hydrogen atoms of the DPM ligands were located and included as fixed contributions but were not refined. Their idealized positions were calculated from the geometries about their attached carbon atoms and C–H distances of 0.95 Å. Hydrogen atoms were assigned isotropic thermal parameters of 1 Å^2 greater than the isotropic thermal parameter (or equivalent isotropic thermal parameter of anisotropic atoms) of their attached carbons. Attempts to locate the hydride ligands by using standard techniques were unsuccessful. The C and O atoms of the carbonyl groups did not refine well anisotropically and so were left isotropic. Close inspection of the electron density maps in the regions of the carbonyl groups did not reveal any evidence of disorder of these groups.

Although the elemental analyses indicated the presence of two CH_2Cl_2 solvent molecules in the asymmetric unit, only ca. 1.2 CH_2Cl_2's were located. Each molecule refined to an occupancy of 0.6, suggesting the disorder of two molecules over three sites, each with an occupancy of ca. two-thirds. A third area of smeared out electron density was located in the cell near the two other partial occupancy CH_2Cl_2 molecules, but attempts to fit this density to one or more CH_2Cl_2 orientations failed; therefore, this density was left unaccounted for. The hydrogen atoms of the solvent molecules were not included owing to the large thermal parameters of the carbon atoms.

Table II. Summary of Crystal Data and Details of Intensity Collection

compd	$[Ir_2(H)(CO)_2(\mu\text{-}H)_2(DPM)_2][Cl]\cdot 1.2CH_2Cl_2$
fw	1349.59
formula	$Ir_2Cl_{3.4}P_4O_2C_{58.2}H_{49.4}$
cell params	
a, Å	12.794 (4)
b, Å	20.468 (5)
c, Å	20.433 (8)
β, deg	91.58 (4)
d(calcd), g/cm^3	1.654
space group	$P2_1/n$ (nonstandard setting of $P2_1/c$, No.14)
temp, °C	22
radiation (λ, Å)	graphite-monochromated Mo Kα (0.71069)
receiving aperature, mm	2.00 + (0.500 tan θ) wide × 4.0 high, 173 from crystal
takeoff angle, deg	3.05
scan speed, deg/min	variable between 10.06 and 0.91
scan width, deg	0.75 + (0.347 tan θ) in ω
2θ limits, deg	$0.20 < 2\theta < 50.00$
no. of unique data collcd	9461 ($+h,+k,\pm l$)
no. of unique data used (F_o^2, $\geqslant 3\sigma$ (F_o^2)) (NO)	3543
cryst shape (four used in data collcn)	monoclinic prism with faces of the form {100}, {010}, {001}
cryst dimens, mm	(1) 0.24 × 0.20 × 0.06 (2) 0.13 × 0.13 × 0.05 (3) 0.18 × 0.16 × 0.05 (4) 0.17 × 0.16 × 0.05
range of transmissn factors	(1) 0.353–0.742 (2) 0.607–0.778 (3) 0.451–0.749 (4) 0.631–0.784
final no. of params refined (NV)	241
error in observn of unit wt[a]	2.367
R[b]	0.080
R_w[c]	0.102

[a] $GOF = [\sum w(|F_o| - |F_c|)^2/(NO - NV)]^{1/2}$. [b] $R = \sum||F_o| - |F_c||/\sum|F_o|$. [c] $R_w = [\sum w(|F_o| - |F_c|)^2/\sum wF_o^2]^{1/2}$.

The final model in space group $P2_1/n$ with 241 parameters refined converged as indicated in Table II. In the final difference Fourier map, the 20 highest residuals (1.4–0.4 e/Å^3) were in the vicinity of the solvent molecules and the Ir atoms. A typical carbon on an earlier synthesis had an electron density of 4.0 e/Å^3. The electron density in the vicinities of the Ir atoms was much too close to the metals to correspond to groups bonded to Ir and could not be attributed to the hydrido ligands. Our failure to locate the hydrido ligands is not surprising considering the unavoidably poor quality of the data. The parameters for the individual, non-hydrogen atoms and those of the rigid groups are given in Tables III and IV,[28] respectively. Tables of anisotropic thermal parameters, the derived hydrogen parameters and a listing of the observed and calculated structure amplitudes are available a Supplementary Material.

Description of Structure

Attempts to obtain X-ray suitable crystals of compound **5** as the BF_4^- salt proved unsuccessful; however, it was isolated in crystalline form with a chloride counterion from the reaction of **3** with CH_2Cl_2. Although the crystals of **5b** were not of ideal quality, they did prove adequate for a determination of the gross structural features. The asymmetric unit of the unit cell contains one molecule of **5b** along with two unexceptional partial occupancy (0.6) CH_2Cl_2 solvent molecules. There are no unusual contacts involving the solvent molecules. The chloride counterion is hydrogen bonded to one of the DPM methylene hydrogens of the dimer (vide infra).

The complex cation, shown in Figure 1 together with the hydrogen-bound chloride ion, appears as a rather typical DPM-bridged complex.[5,7] Both DPM ligands bridge the two metals in essentially mutually trans positions about the metals, and the orientations of the phenyl groups are such as to minimize nonbonded contacts with the ligands in the equatorial plane. Therefore, four phenyl groups (2, 3, 5, and 7) are thrust into the relatively vacant positions on the side of the complex opposite the carbonyl group C(1)O(1) (see Figure 1).

Although the hydride ligands were not crystallographically located, their approximate positions are obvious based on the

---

(10) Doedens, R. J.; Ibers, J. A. *Inorg. Chem.* **1967**, *6*, 204.
(11) For the programs used in structure solution and refinement, see ref 7.
(12) Cromer, D. T.; Waber, J. T. *International Tables for Crystallography*; Kynoch: Birmingham, England, 1974; Vol. IV, Table 2.2 A.
(13) Stewart, R. F.; Davidson, E. R.; Simpson, W. T. *J. Chem. Phys.* **1965**, *42*, 3175.
(14) Cromer, D. T.; Liberman, D. J. *J. Chem. Phys.* **1970**, *53*, 1891.

Table III. Positional and Thermal Parameters of the Non Rigid Group Atoms of $[Ir_2(H)(CO)_2(\mu\text{-}H)_2(DPM)_2][Cl]\cdot 1.2CH_2Cl_2$

atom	x^a	y	z	B, Å^2	atom	x	y	z	B, Å^2
Ir(1)	0.0633 (1)	0.30591 (7)	0.20873 (7)	3.08^b	P(4)	−0.1099 (7)	0.1626 (4)	0.1752 (5)	2.8^b
Ir(2)	0.0582 (1)	0.18299 (6)	0.14266 (7)	2.90^b	O(1)	0.080 (2)	0.322 (1)	0.356 (2)	9.0 (7)
Cl(1)	−0.4333 (8)	0.1977 (6)	0.2644 (6)	6.1^b	O(2)	0.042 (2)	0.074 (1)	0.049 (2)	6.3 (7)
Cl(2)^c	0.0401 (19)	0.1196 (15)	0.3622 (11)	12.7^b	C(1)	0.079 (3)	0.324 (2)	0.300 (2)	7.3 (9)
Cl(3)	0.2401 (27)	0.1520 (16)	0.3429 (13)	15.0^b	C(2)	0.047 (3)	0.117 (2)	0.078 (2)	4.3 (9)
Cl(4)	0.5118 (24)	0.0676 (22)	0.4394 (16)	18.5^b	C(3)	0.305 (2)	0.242 (2)	0.182 (2)	2.9^b
Cl(5)	0.4708 (57)	0.0071 (29)	0.3544 (28)	22.9^b	C(4)	−0.157 (3)	0.221 (2)	0.234 (2)	3.4^b
P(1)	0.2423 (7)	0.3199 (5)	0.1958 (5)	3.4^b	C(5)	0.151 (5)	0.095 (3)	0.312 (4)	7.7 (17)
P(2)	0.2318 (6)	0.1953 (5)	0.1178 (4)	3.2^b	C(6)	0.474 (6)	0.097 (4)	0.367 (4)	8.6 (20)
P(3)	−0.1183 (6)	0.3028 (4)	0.2143 (4)	2.7^b					

^{a} Estimated standard deviations of this and other tables are given in parentheses and correspond to the least significant digits. ^{b} Equivalent isotropic thermal parameter for anisotropic atom. ^{c} The solvent molecules are labeled as follows: for $CH_2Cl_2(1)$, C(5), Cl(2), Cl(3); for $CH_2Cl_2(2)$, C(6), Cl(4), Cl(5).

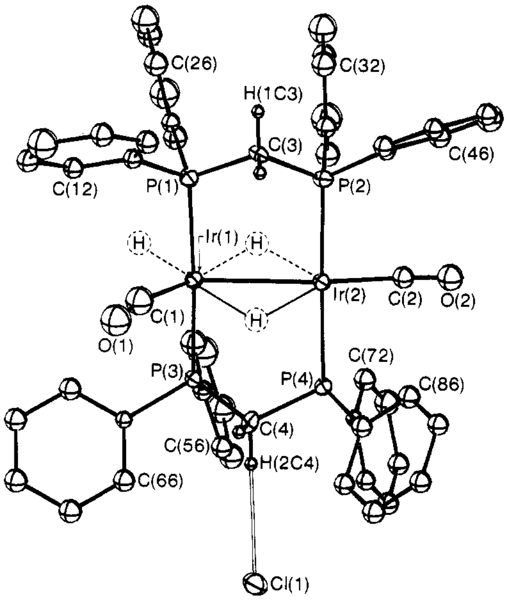

Figure 1. Perspective view of $[Ir_2H(CO)_2(\mu\text{-}H)_2(DPM)_2][Cl]$. Hydrido ligands, which were not located, are shown in their idealized positions. Thermal ellipsoids are drawn at the 20% level except those for methylene hydrogens, which are drawn artificially small. Phenyl hydrogens have the same number as their attached carbon atoms.

Table V. Selected Distances (Å) in $[Ir_2(H)(CO)_2(\mu\text{-}H)_2(DPM)_2][Cl]^a$

	Bond Distances		
Ir(1)–Ir(2)	2.855 (2)	P(2)–C(3)	1.85 (3)
Ir(1)–C(1)	1.91 (4)	P(3)–C(4)	1.79 (3)
Ir(1)–P(1)	2.331 (9)	P(4)–C(4)	1.82 (4)
Ir(1)–P(3)	2.330 (8)	P(1)–C(11)	1.81 (2)
Ir(2)–C(2)	1.90 (4)	P(1)–C(21)	1.80 (2)
Ir(2)–P(2)	2.306 (9)	P(2)–C(31)	1.85 (2)
Ir(2)–P(4)	2.307 (9)	P(2)–C(41)	1.81 (2)
Cl(1)–H(2C4)	2.65	P(3)–C(51)	1.81 (2)
Cl(1)–O(1)	1.15 (4)	P(3)–C(61)	1.81 (2)
C(2)–O(2)	1.05 (4)	P(4)–C(71)	1.83 (2)
P(1)–C(3)	1.82 (3)	P(4)–C(81)	1.86 (2)
	Nonbonded Distances		
P(1)–P(3)	3.01 (1)	C(2)–H(72)	2.74
P(2)–P(4)	2.98 (1)	C(2)–H(86)	2.76
O(1)–H(74)^b	2.49	O(2)–H(86)	2.89

^{a} Interatomic distances and angles for the CH_2Cl_2 solvent molecules are listed in the supplementary material. ^{b} Molecule at $-^1/_2 + x$, $^1/_2 - y$, $-^1/_2 + z$

positions of the other ligands in the structure and on the spectroscopic data observed for **5**. The ^1H NMR spectrum clearly indicates that two hydride ligands bridge the metals (probably on opposite faces of the complex) while another is terminal (vide infra). Location of the terminal hydride ligand becomes obvious upon examining the geometries about each metal. The carbonyl group C(2)O(2) is almost linearly disposed along the Ir–Ir bond (Ir(1)–Ir(2)–C(2) angle = 164 (1)°) whereas the group C(1)O(1) is bent away from this vector, forming an Ir(2)–Ir(1)–C(1) angle of 129 (1)° and leaving a conspicuosly vacant coordination site on Ir(1) adjacent to C(1). Clearly the terminal hydride ligand must occupy this coordination site as diagrammed below, and **5** can be thought of as the protonated iridium analogue of $[Rh_2(CO)_2(\mu\text{-}H)_2(DPM)_2]$, which has been previously reported.[15]

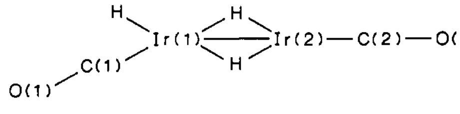

The resulting coordination geometries about each metal differ significantly. If the formal metal–metal bond is ignored, the geometry about Ir(1) is pseudooctahedral whereas that about Ir(2) more closely approximates a trigonal bipyramid. Although the metal–phosphorus distances are normal, they can be grouped into two pairs, with those on Ir(1) (average 2.331 (9) Å) being slightly longer than those on Ir(2) (average 2.307 (9) Å). This difference is barely significant; nevertheless, the two metal–phosphorus distances on each metal are in excellent mutual agreement, and the difference is consistent with the different coordination numbers of the metals. We have previously observed in similar cases that the longer metal–phosphorus distances are associated with the metal having the higher coordination number.[16,17] The carbonyl geometries are normal; the slight bend in these groups, (166 (4)° and 170 (4)°) is not unusual and most probably results from nonbonded contacts involving phenyl groups 7 and 8 (see Figure 1 and Table VI). Similar bending of the carbonyl groups was observed in the two independent molecules of $[Rh_2Cl_2(CO)(C_2S_4)(DPM)_2]$, and again, short nonbonded phenyl contacts were responsible.[18]

The Ir–Ir separation (2.855 (2) Å) is normal for a single bond and is consistent with the range of values observed for other Ir–Ir-bonded DPM-bridged systems.[5,19-21] This metal–metal distance is significantly shorter than the intraligand P···P separation (average 3.00 (1) Å) indicating compression along the Ir–Ir axis and mutual attraction of the metals. It should be noted, however, that in the presence of the bridging hydride groups the Ir–Ir bond order is not unambiguous.

As noted earlier, the chloride ion is hydrogen bound to H(2C4) of one of the DPM ligands, at a distance of approximately 2.7 Å. This contact is somewhat uncertain since the hydrogen atom was included in the idealized position for an unperturbed CH_2 group, at 0.95 Å from carbon, and was not refined; nevertheless, it indicates a substantial interaction. We have previously observed

---

(15) Woodcock, C.; Eisenberg, R. *Inorg. Chem.* **1984**, *23*, 4207.

(16) Sutherland, B. R.; Cowie, M. *Inorg. Chem.* **1984**, *23*, 1290.

(17) Gibson, J. A. E.; Cowie, M. *Organometallics* **1984**, *3*, 722.

(18) Cowie, M., Dwight, S. K. *J. Organomet. Chem.* **1981**, *214*, 233.

(19) Sutherland, B. R.; Cowie, M. *Organometallics* **1984**, *3*, 1869.

(20) Kubiak, C. P.; Woodcock, C.; Eisenberg, R. *Inorg. Chem.* **1980**, *19*, 2733.

(21) Sutherland, B. R.; Cowie, M. *Can. J. Chem.* **1986**, *64*, 464.

Table VI. Selected Angles (deg) in $[Ir_2(H)(CO)_2(\mu\text{-}H)_2(DPM)_2][Cl]$

Ir(2)–Ir(1)–C(1)	129.2 (12)	Ir(1)–P(1)–C(3)	110.4 (10)	C(3)–P(2)–C(31)	106.2 (12)	P(1)–C(21)–C(22)	119.1 (11)
Ir(2)–Ir(1)–P(1)	93.7 (2)	Ir(2)–P(2)–C(3)	111.9 (10)	C(3)–P(2)–C(41)	103.0 (12)	P(1)–C(21)–C(26)	120.8 (10)
Ir(2)–Ir(1)–P(3)	89.4 (2)	Ir(1)–P(3)–C(4)	108.8 (12)	C(4)–P(3)–C(51)	107.8 (13)	P(2)–C(31)–C(32)	123.3 (11)
P(1)–Ir(1)–C(1)	90.7 (12)	Ir(2)–P(4)–C(4)	113.8 (11)	C(4)–P(3)–C(61)	105.4 (12)	P(2)–C(31)–C(36)	116.6 (11)
P(3)–Ir(1)–C(1)	91.9 (12)	Ir(1)–P(1)–C(11)	115.6 (7)	C(4)–P(4)–C(71)	105.4 (12)	P(2)–C(41)–C(42)	120.7 (9)
P(1)–Ir(1)–P(3)	173.4 (3)	Ir(1)–P(1)–C(21)	118.5 (8)	C(4)–P(4)–C(81)	98.2 (12)	P(2)–C(41)–C(46)	119.2 (10)
Ir(1)–Ir(2)–C(2)	163.6 (12)	Ir(2)–P(2)–C(31)	118.0 (8)	C(11)–P(1)–C(21)	100.1 (10)	P(3)–C(51)–C(52)	120.8 (10)
Ir(1)–Ir(2)–P(2)	89.9 (2)	Ir(2)–P(2)–C(41)	116.4 (6)	C(31)–P(2)–C(41)	99.8 (11)	P(3)–C(51)–C(56)	119.2 (10)
Ir(1)–Ir(2)–P(4)	91.9 (2)	Ir(1)–P(3)–C(51)	118.7 (7)	C(51)–P(3)–C(61)	101.2 (10)	P(3)–C(61)–C(62)	118.8 (9)
P(2)–Ir(2)–C(2)	88.9 (12)	Ir(1)–P(3)–C(61)	114.0 (7)	C(71)–P(4)–C(81)	105.7 (9)	P(3)–C(61)–C(66)	121.3 (8)
P(4)–Ir(2)–C(2)	90.9 (12)	Ir(2)–P(4)–C(71)	116.7 (6)	P(1)–C(3)–P(2)	110.3 (4)	P(4)–C(71)–C(72)	118.5 (8)
P(2)–Ir(2)–P(4)	174.1 (3)	Ir(2)–P(4)–C(81)	115.0 (7)	P(2)–C(4)–P(4)	111.2 (4)	P(4)–C(71)–C(76)	121.5 (8)
Ir(1)–C(1)–O(1)	166 (4)	C(3)–P(1)–C(11)	103.0 (12)	P(1)–C(11)–C(12)	117.0 (10)	P(4)–C(81)–C(82)	121.8 (9)
Ir(2)–C(2)–O(2)	170 (4)	C(3)–P(1)–C(21)	107.8 (12)	P(1)–C(11)–C(16)	122.6 (9)	P(4)–C(81)–C(86)	118.2 (10)

Scheme I

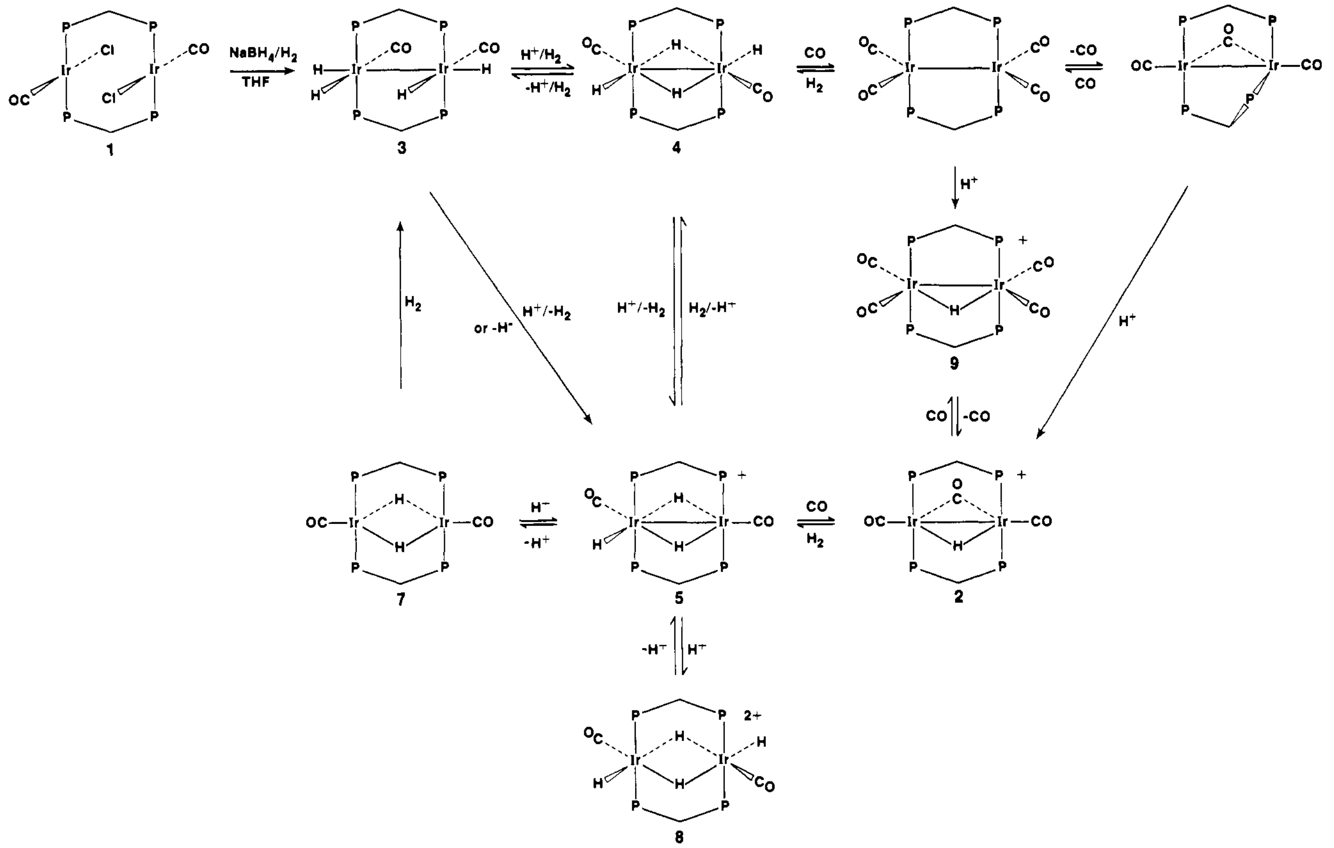

hydrogen bonding between a DPM methylene proton and the chloride ion in $[Ir_2(CO)_2(\mu\text{-}OH\cdot Cl)(DPM)_2]$[5] so this in itself is not surprising. However, what is surprising is that the chloride ion does not coordinate to one of the metal centers in this cationic complex; presumably, this reflects the inertness of the metals in **5** toward attack by nucleophiles.

Results and Discussion

The transformations observed or discussed in this work are summarized in Scheme I. The reaction of *trans*-$[IrCl(CO)(DPM)]_2$ (**1**) with an excess of $NaBH_4$ under H_2 gives rise to a new compound **3** with the formula $[Ir_2(H)_4(CO)_2(DPM)_2]$. The high-field region of the ^1H NMR spectrum shows only two complex multiplets, which could in principle arise from either bridging or terminal hydride ligands. However, the fact that both peaks have almost identical shapes and integrate as two hydrogens each, combined with the observation of terminal Ir–H stretches at 2076 and 2107 cm^{-1} in the infrared spectrum suggests that all of the hydride ligands are terminal. The deuteriated analogue, $[Ir_2(D)_4(CO)_2(DPM)_2]$, showed the carbonyl stretches at 1966 and 1917 cm^{-1} (KBr disc), but no evidence of the Ir–D stretches was obvious; presumably, these were obscured by the strong absorptions due to the phosphine groups. The $^{31}P\{^1H\}$ NMR spectrum shows only a singlet over the temperature range +25 to −60 °C, indicative of a symmetrical species. On the basis of this information, two structures are possible for **3**. The first, shown in Scheme I, in which the carbonyls are mutually cis, has C_{2v} symmetry, while the isomer having the carbonyls in mutually trans positions has C_{2h} symmetry. The cis structure would appear to be the correct choice based on the observation of two ν(CO) bands in the infrared spectrum and two DPM methylene resonances in the room-temperature ^1H NMR spectrum; for the trans structure only one methylene resonance would be expected.[22] However, on the basis of the reaction of **3** with trityl cation (vide infra), the trans configuration cannot be unambiguously ruled out. The phosphorus–hydride couplings ($^2J_{P\text{-}H}$ and $^3J_{P\text{-}H}$) were not resolved; however, in the $^1H\{^{31}P\}$ NMR spectrum of **3** the hydride resonances are resolved to identical doublets ($^2J_{H\text{-}H}$ = 4.7 Hz). Lowering the temperature to −80 °C produced no noticeable effect on the peak shapes, arguing against a fluxional process.

A dihydrogen atmosphere is not necessary in the synthesis. If the reaction is performed under N_2, **3** is still the major product

---

[22] Although the two methylene protons are inequivalent in the static structure, it is expected that they would interchange readily in solution. See: Puddephatt, R. J.; Azam, K. A.; Hill, R. H.; Brown, M. P.; Nelson, C. D.; Moulding, R. P.; Seddon, K. R.; Grossel, M. C. *J. Am. Chem. Soc.* **1983**, *105*, 5642.

formed, but the yield is slightly lower and the reaction time is longer. If, however, the reaction of **1** with $NaBH_4$ is done under a CO atmosphere, the only product observed after 24 h is the previously characterized Ir(0) compound $[Ir_2(CO)_4(DPM)_2]$.[5] This latter product and the related compound $[Ir_2(CO)_3(DPM)_2]$,[5] are the major species formed when a solution of **3** is allowed to stir under CO for 24 h, so these Ir(0) species apparently result from reductive substitution[23] of the hydride ligands by CO. It is not clear how substitution of H_2 by CO in compound **3** occurs, since this compound is coordinatively saturated. The reverse oxidative addition of H_2 to $[Ir_2(CO)_3(DPM)_2]$ gives mainly **3** after 24 h. Although **3**, $[Ir_2(CO)_3(DPM)_2]$, and $[Ir_2(CO)_4(DPM)_2]$ are not the only species observed in these reactions, the other minor products are present in small concentrations and their identification has not been possible. Reaction of compound **3** with 1 or 2 equiv of PMe_3 yields mixtures of products that have so far escaped identification and characterization and does not appear to induce the same reductive substitution of the hydride ligands as does CO.

The formation of **3** from the reaction of *trans*-$[IrCl(CO)(DPM)]_2$ with $NaBH_4$ is in contrast to the reaction involving the Rh analogue, in which the dihydride species $[Rh_2(CO)_2(\mu\text{-}H)_2(DPM)_2]$ was isolated under an H_2 atmosphere.[15] Although we do not observe the analogous iridium dihydride in our reactions using $NaBH_4$, we have successfully prepared this species by another route (vide infra).

The reaction of **3** with $HBF_4 \cdot Et_2O$ gives two different products depending on whether or not an H_2 atmosphere is present (see Scheme I). Under H_2 compound **3** immediately rearranges in the presence of strong acid to the isomer $[Ir_2(H)_2(CO)_2(\mu\text{-}H)_2(DPM)_2]$ (**4**). Although we were unable to obtain IR characterization of this species, due to its reaction with the IR cells used, its NMR characterization seems straightforward. The $^{31}P\{^1H\}$ NMR spectrum shows a singlet, indicating that all phosphorus nuclei are chemically equivalent, and the ^1H NMR spectrum shows a quintet due to the two bridging hydrides, coupled to all four phosphorus nuclei, and a broad unresolved resonance for the two equivalent terminal hydrides. In all symmetrical species having terminal hydride groups, we have observed that these resonances are broadened and complex, if not unresolved. When 1 equiv of CF_3CO_2H is used to effect the isomerization of **3** to **4**, a single resonance, integrating as one proton and assigned to free CF_3CO_2H, is observed at 10.64 ppm. This assignment is confirmed by the observed growth of this resonance upon addition of excess CF_3CO_2H. The acid-catalyzed isomerization of **3** to **4** can be reversed upon neutralization of the acid by the addition of $KOC(CH_3)_3$. All attempts to isolate compound **4** as a solid resulted in mixtures of species, one major product being **5** (vide infra). Weaker acids than $HBF_4 \cdot Et_2O$ or CF_3CO_2H can be used to accomplish the protonation of **3**. Both H_2O and MeOH, when added to solutions of **3** under H_2, produce **4** as observed in the $^{31}P\{^1H\}$ NMR spectrum. However, even in the presence of 100–200-fold excesses of these weak acids, only 5–10% of **4** was observed by NMR after 24 h.

If the reaction of **3** with $HBF_4 \cdot Et_2O$ is performed under an atmosphere of nitrogen instead of hydrogen, the solution begins to darken after several minutes and a new complex pattern typical of an unsymmetrical species appears in the $^{31}P\{^1H\}$ NMR spectrum. After the mixture is stirred overnight, only this latter pattern is observed. The reaction can be accelerated by slowly bubbling N_2 through the solution. Adding ether to the solution leads to the isolation of a golden yellow solid, **5a**, whose solution and solid spectroscopic parameters (see Table I) indicate that it is the cationic trihydride shown in Scheme I. The ^1H NMR spectrum of compound **5a**, in the region of the hydride resonances, is shown in Figure 2A. The high-field resonance is that of the terminal hydride ligand split into a triplet by the two adjacent phosphorus nuclei. Surprisingly perhaps there is no obvious coupling to the bridging hydride ligand, which is trans to this terminal one; any such coupling must be less than ca. 5 Hz (the width at half-height of each peak of the triplet). Both bridging hydride resonances are complex due presumably to coupling to the two sets of inequivalent P nuclei and bridged H–H coupling. No evidence of the bridging hydride or deuteride groups was observed in the IR spectra of the hydrido or deuterido complexes. Confirmation of this proposed structure comes from the crystal structure determination of this compound with a chloride counterion (**5b**) (see Figure 1). It seems probable that both compounds **4** and **5** result from an unobserved cationic pentahydride intermediate $[Ir_2(H)_5(CO)_2(DPM)_2]^+$ (**6**); in the presence of H_2, loss of H^+ results, yielding **4**, whereas in the absence of H_2, hydrogen loss occurs, yielding **5**.

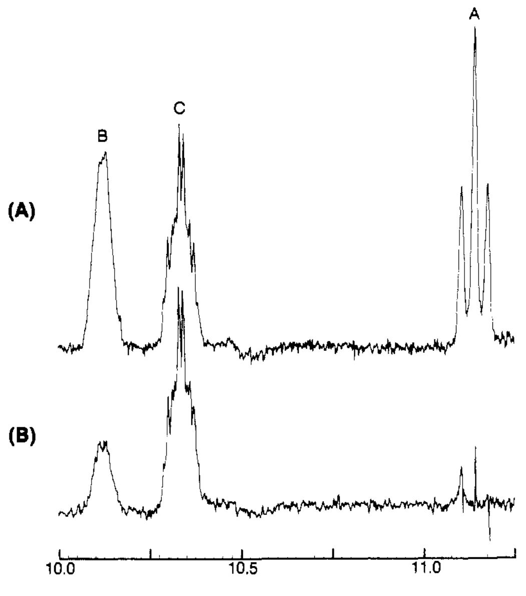

Figure 2. (A) ^1H NMR spectrum at 400 MHz of $[Ir_2(H)(CO)_2(\mu\text{-}H)_2(DPM)_2][BF_4]$ (**5a**) in the region of the hydride resonances. (B) Spin-saturation transfer experiment. The spectral region is as in spectrum A but with irradiation of resonance A at −11.1 ppm.

Compound **5** can also be produced by H^- abstraction from **3** using trityl cation (see Experimental Section), and conversely, reaction of **5** with sodium borohydride regenerates **3** as the only observed product. Although these observations suggest the trans geometry for **3** (C_{2h} geometry), rearrangement of the initial products is not unlikely.

A spin-saturation transfer experiment performed by irradiating the terminal hydride resonance in the ^1H NMR spectrum of **5** indicates that it and one of the bridging hydrides are undergoing site exchange. This can be seen in Figure 2B, in which the disappearance of the terminal-hydride resonance A is accompanied by a 70% reduction in the intensity of bridging-hydride resonance B. The other bridging-hydride signal remains unchanged. This observation can be rationalized in terms of the process

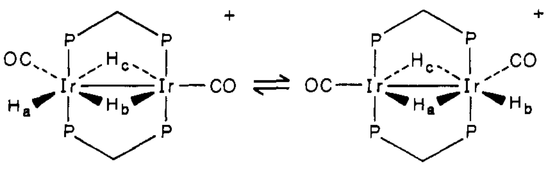

This interchange is slow on the NMR time scale since both the $^{31}P\{^1H\}$ and ^1H NMR spectra are sharp at room temperature and no averaging of the signals due to H_a and H_b is observed.

An alternative method for the preparation of **5** is the reaction of **3** with chlorinated solvents such as CH_2Cl_2 or $CHCl_3$, yielding **5b** (with a Cl^- counterion). Compound **5b** is virtually identical with **5a** in its NMR and IR spectroscopic properties. This transformation is notable in that, unlike the hydride–chloride exchange reactions of many other polyhydride complexes, only one of the four hydride ligands of **4** is replaced by a chloride ion. In addition, the X-ray structure determination indicates that this

---

[23] The term reductive substitution describes an apparent overall result; no mechanistic implications are being made.

chloride ion is not bound to the coordinatively unsaturated Ir center but is instead associated with one of the DPM methylene hydrogens. This appears to be true in solution as well, as evidenced by the low conductivity values observed in both CH_2Cl_2 (10.4 Ω^{-1} cm^2 mol^{-1}) and nitromethane (26.2 Ω^{-1} cm^2 mol^{-1}). The lack of association of chloride ions to a metal center is surprising and seems to indicate a reduced degree of metal electrophilicity.

Attempts at deprotonating **5** to give a neutral dihydride species by using nitrogen bases have been unsuccessful; the addition of NEt_3 or proton sponge[9] produced no change in the $^{31}P\{^1H\}$ NMR spectra even when used in large excess (~200 molar equiv). However, use of the very strong base potassium *tert*-butoxide results in successful deprotonation to give $[Ir_2(CO)_2(\mu\text{-}H)_2(DPM)_2]$ (**7**). Compound **7** appears as a singlet in the $^{31}P\{^1H\}$ NMR spectrum over a range of temperatures between −80 and +20 °C and shows a high-field quintet in the ^1H NMR spectrum, indicating that both hydride ligands are coupled to all four phosphorus nuclei. Protonation of **7** with 1 equiv of $HBF_4\cdot Et_2O$ regenerates **5**, while reaction of **7** with H_2 produces **3**. Compound **7** appears to be the iridium analogue of the previously reported rhodium species.[15] Although coupling of the hydride resonances to the phosphorus nuclei was apparently not observed in the Rh compound, this is clearly seen in our Ir species. A potentially more direct route to **7**, that of reacting $[IrCl(CO)(DPM)]_2$ (**1**) with 2 equiv of the single hydride source $LiB(C_2H_5)_3H$, was unsuccessful and led only to a mixture of unidentified products.

The reaction of **5a** with a 3-fold excess of $HBF_4\cdot Et_2O$ under N_2 results in the precipitation of the highly insoluble white compound **8**. The $^{31}P\{^1H\}$ NMR spectrum of **8** shows a singlet even at low temperatures, while the high-field region of the ^1H NMR spectrum shows two poorly resolved broad resonances of equal intensity at δ −9.20 and −19.22 (it is not possible to determine the multiplicities of these peaks since the very low solubility resulted in a very poor signal to noise ratio). On the basis of this evidence and the IR spectral data, which shows one terminal CO band and one terminal Ir–H band, compound **8** has been assigned the structure shown in Scheme I. Again, no evidence of bridging hydride or deuteride ligands appears in the IR spectra of the hydride or deuteride complexes. Compound **8** is deprotonated in acetone solution, showing ca. 50% proton loss after several minutes (by infrared) and complete deprotonation after 1 h, regenerating **5**. Conversely, the protonation of **5** to produce **8** could not be accomplished when weaker acids such as HCl or MeOH were employed. The tendency of **8** to deprotonate and its insolubility in most solvents led to the use of nitromethane as the solvent for NMR characterization and conductivity measurements. Compound **8** has also been shown to reductively eliminate H_2 when reacted with CO; after ca. 15 min, the ^1H and $^{31}P\{^1H\}$ NMR spectra show that the exclusive product is the previously characterized $[Ir_2(CO)_4(\mu\text{-}H)_2(DPM)_2][BF_4]_2$.[5]

The reaction of compound **5a** with CO does not lead directly to the expected $[Ir_2(CO)_2(\mu\text{-}H)(\mu\text{-}CO)(DPM)_2][BF_4]$ but instead yields a major product that appears as a sharp singlet at −9.6 ppm in the $^{31}P\{^1H\}$ NMR spectrum. When the solution is flushed with N_2, this resonance disappears, being replaced by the singlet at 9.1 ppm due to the expected product. Flushing CO through this latter solution regenerates the initial major product. On the basis of these results, the ^1H NMR spectrum (which shows a quintet in the hydride region), and the IR spectrum (which shows no bridging CO stretches), we have identified the major product as $[Ir_2(CO)_4(\mu\text{-}H)(DPM)_2][BF_4]$ (**9**), which has been subsequently prepared by more direct methods (see Experimental Section). The reverse process, reaction of $[Ir_2(CO)_2(\mu\text{-}H)(\mu\text{-}CO)(DPM)_2][BF_4]$ with hydrogen to produce **5a**, goes to completion within 24 h.

Although all of the polyhydride complexes described herein are proposed as classical hydrides, the possibility of molecular hydrogen complexes was considered but was rejected for a number of reasons. The complexes are thermally stable under an N_2 atmosphere for at least several days and may be dried in vacuo with no apparent H_2 loss, arguing against the presence of a presumably labile $\eta^2\text{-}H_2$ ligand. In the ^1H NMR spectra of these compounds the hydride signals appear as complex multiplets rather than broad, featureless resonances as seem typical for the H_2 complexes.[24-26] Furthermore, inversion–recovery NMR experiments show apparent relaxation times (T_1) of the hydride resonances to be within the range 0.29–0.58 s, comparable to those observed in other studies[26,27] and an order of magnitude greater than those expected for a dihydrogen ligand signal.[26]

Summary

The reaction of *trans*-$[IrCl(CO)(DPM)]_2$ (**1**) with $NaBH_4$ proceeds quite unlike that involving the analogous rhodium complex. Whereas the only rhodium hydride species isolated in this reaction, $[Rh(CO)(\mu\text{-}H)(DPM)]_2$, apparently results from a simple metathasis reaction (H^- for Cl^-), this does not occur for iridium and a variety of iridium hydrides is ultimately obtained, as shown in Scheme I. With iridium the bridging dihydride is not obtained directly, and instead the tetrahydride $[Ir(CO)(H)_2(DPM)]_2$ (**3**) results. The analogous dihydride $[Ir(CO)(\mu\text{-}H)(DPM)]_2$ can however be obtained from **3** by successive hydride loss and deprotonation steps. This reactive and coordinatively unsaturated dihydride species is of great interest, since, as noted, it is the binuclear iridium analogue of the proposed intermediate in hydroformylation catalysis, $[RhH(CO)(PPh_3)_2]$, and studies with this binuclear dihydride are under way. Similarly the chemistry of the other hydride species with unsaturated organic substrates is also being pursued in hope of gaining information on the nature of the involvement of adjacent metal centers in catalysis by metal hydrides. These complexes are especially relevant to such studies since apart from the bridging diphosphine groups holding the metals together, only hydride and carbonyl ligands are present, both of which are catalytically interesting groups.

Acknowledgment. This work was supported by the University of Alberta and the Natural Sciences and Engineering Research Council of Canada. We thank the NSERC for a graduate scholarship to B.R.S., Dr. R. G. Ball for collecting the X-ray data, and Johnson Matthey for a generous loan of $IrCl_3\cdot 3H_2O$.

Registry No. **1**, 66125-35-7; **2**, 97487-43-9; **3**, 110014-66-9; **4**, 110014-67-0; **5a**, 110014-69-2; **5b**, 110014-71-6; **7**, 110014-72-7; **8**, 110014-74-9; **9**, 110026-35-2; $[Ir_2(CO)_4(DPM)_2]$, 97487-40-6; HBF_4, 16872-11-0; $Ph_3C^+BF_4^-$, 341-02-6; $CHCl_3$, 67-66-3; CH_2Cl_2, 75-09-2; $KOC(CH_3)_3$, 865-47-4; $NaBH_4$, 16940-66-2; Ir, 7439-88-5.

Supplementary Material Available: Tables of thermal parameters for the anisotropic atoms, idealized hydrogen parameters, bond distances and angles for the solvent molecules, and derived parameters for the rigid group atoms (Table IV) (5 pages); a listing of observed and calculated structure amplitudes (11 pages). Ordering information is given on any current masthead page.

---

(24) Kubas, G. J.; Ryan, R. R.; Swanson, B. I.; Vergamini, P. J.; Wasserman, H. J. *J. Am. Chem. Soc.* **1984**, *106*, 451.

(25) Morris, R. H.; Sawyer, J. F.; Shiralian, M.; Zubkowski, J. D. *J. Am. Chem. Soc.* **1985**, *107*, 5581.

(26) Crabtree, R. H.; Lavin, M.; Bonneviot, L. *J. Am. Chem. Soc.* **1986**, *108*, 4032.

(27) Crabtree, R. H.; Segmuller, B. E.; Uriarte, R. J. *Inorg. Chem.* **1985**, *24*, 1949.

(28) Supplementary material.